SOLAR NEUTRINOS

A.B. McDonald
SNO Institute, Queen's University
Kingston, Ontario, Canada

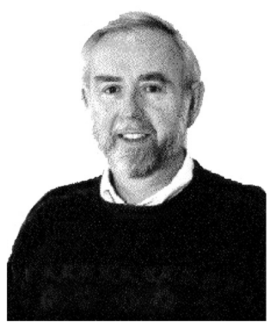

ABSTRACT

Present results and future measurements of solar neutrinos are discussed. The results to date indicate that solar electron neutrinos are changing to other active types and that transitions solely to sterile neutrinos are disfavored. The flux of ^8B solar neutrinos produced in the Sun, inferred assuming only active neutrino types, is found to be in very good agreement with solar model calculations. Future measurements will focus on greater accuracy for charged current and neutral current sensitive reactions to provide more accurate measurements of neutrino flavor change and further studies of day-night flux differences and spectral shape. Other experiments sensitive to lower energy solar neutrinos will be in operation soon.

1 Present Status of Solar Neutrino Experiments

Starting the 1960's with the pioneering experiments of Davis and his collaborators [1] using Chlorine as a solar neutrino detection medium, a discrepancy was identified between the experimental measurements and the theoretical calculations [2, 3] for solar neutrino fluxes. Table 1 lists the results for neutrino fluxes from experiments up to the year 2000 and compares them with solar model calculations. The rates are factors of two or three lower than predictions in each case, leading to the conclusion that either solar models are incomplete or there are processes occurring such as flavor change to neutrino types for which the experiments have little or no sensitivity. This 30-year old discrepancy had come to be known as the "Solar Neutrino Problem".

Many attempts have been made to understand these discrepancies in terms of modifications to the solar model, without significant success. The results may be understood in terms of neutrino flavor change in vacuum or with matter enhancement in the sun[4]. However, clear interpretation in terms of neutrino flavor change depends upon solar models because the various experiments have different thresholds and are sensitive to different combinations of the nuclear reactions in the sun. Therefore solar model-independent approaches have also been pursued experimentally to seek an unambiguous indication of flavor change. These approaches have included searches for spectral distortion, day-night and seasonal flux differences by Super-Kamiokande[5, 6]. These measurements are accurate but have provided no clear indication of flavor change to date.

The possible effect of neutrino flavor regeneration in the earth after flavor change in the Sun has been studied through the day-night asymmetry, defined as $\mathcal{A} = (\Phi_n - \Phi_d)/\Phi_{average}$, where $\Phi_{average} = \frac{1}{2}(\Phi_n + \Phi_d)$. The Super-Kamiokande results for ^8B neutrinos [6] are:

$$\mathcal{A} = 0.021 \pm 0.021 \text{ (stat.)}^{+0.013}_{-0.012} \text{ (sys.)}$$

showing no clear indication of regeneration. Figure 1 shows the dependence of the solar neutrino flux measured by Super-Kamiokande [5] on zenith angle as well as the day-night comparison. Studies by Super-Kamiokande of seasonal variations also show no evidence for effects other than detected rate changes arising from the eccentricity of the earth's orbit[6].

The recent measurements[7, 8] by the Sudbury Neutrino Observatory (SNO) of interactions of ^8B solar neutrinos in a heavy water detector provide a solar-model-independent measurement of neutrino flavor change by comparing charged current (CC) and neutral current (NC) interactions with deuterium. The Charged Current

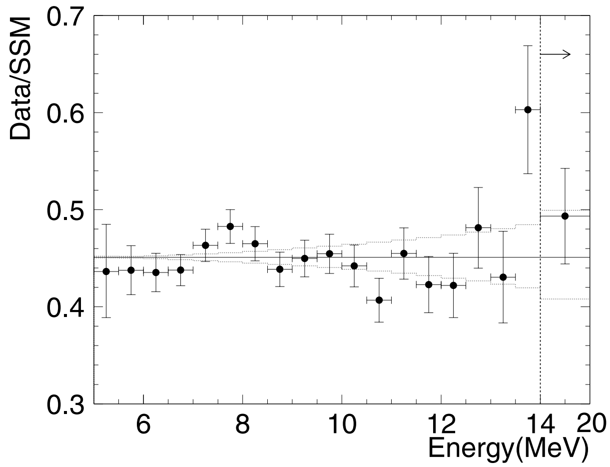

Figure 1: The measured ^{8}B + *hep* solar neutrino spectrum from Super-Kamiokande [5] relative to that of Ortiz *et al.* normalized to the SSM [2]. The data from 14 MeV to 20 MeV are combined into a single bin. The horizontal solid line shows the measured total flux, while the dotted band around this line indicates the energy correlated uncertainty. Error bars show statistical and energy-uncorrelated errors added in quadrature.

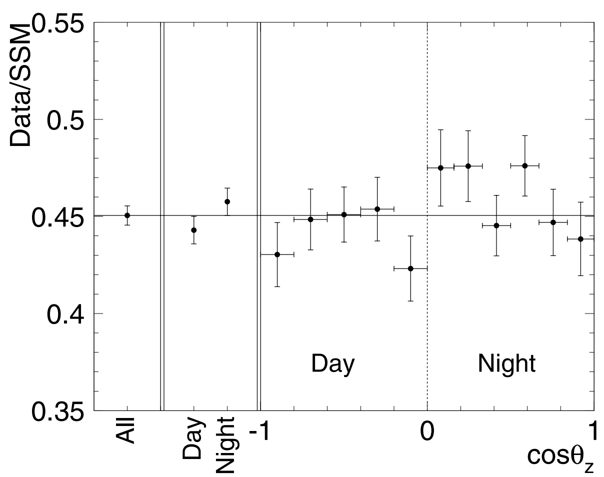

Figure 2: The solar zenith angle (θ_z) dependence of the solar neutrino flux measured by Super-Kamiokande(error bars show statistical error). The width of the night-time bins was chosen to separate solar neutrinos that pass through the Earth's dense core ($\cos\theta_z \geq 0.84$) from those that pass through the mantle ($0 < \cos\theta_z < 0.84$). The horizontal line shows the flux for all data.

Table 1: Summary of solar neutrino observations at different solar neutrino detectors. Homestake, SAGE, Gallex, and GNO fluxes are quoted in units of SNU. The Kamiokande and Super-Kamiokande flux measurements are quoted in units of 10^6 cm^{-2} s^{-1}.

Experiment	Measured Flux	SSM Flux [2]	Ref.
Homestake	2.56 ± 0.16(stat.)±0.16(sys.)	$7.6^{+1.3}_{-1.1}$	[1]
SAGE	$70.8^{+5.3}_{-5.2}$(stat.+sys.)	128^{+9}_{-7}	[10]
Gallex	77.5 ± 6.2(stat.)±4.5(sys.)	128^{+9}_{-7}	[11]
GNO	65.2 ± 6.4(stat.)±3.0(sys.)	128^{+9}_{-7}	[12]
Kamiokande	2.80 ± 0.19(stat.)±0.33(sys.)	$5.05\left(1^{+0.20}_{-0.16}\right)$	[9]
Super-Kamiokande	$2.35\pm$ 0.025(stat.)$^{+0.07}_{-0.06}$(sys.)	$5.05\left(1^{+0.20}_{-0.16}\right)$	[6]

(CC) reaction

$$d + \nu_e \rightarrow p + p + e^- \tag{1}$$

is specific to electron neutrinos, whereas the Neutral Current (NC) Reaction:

$$\nu_x + d \rightarrow n + p + \nu_x \tag{2}$$

is sensitive to all non-sterile neutrino types equally.

The Elastic Scattering (ES) reaction on electrons:

$$\nu_x + e^- \rightarrow e^- + \nu_x \tag{3}$$

is also sensitive to non-sterile neutrino types other than electron neutrinos, although they have about six times smaller cross section than electron neutrinos. Therefore, another solar-model-independent measurement of neutrino flavor change can be obtained by comparing the CC interactions with the ES interactions.

The SNO collaboration have recently reported results from 306 live days of data with pure heavy water as a detection medium[7]. The flux of ν_e's from ^{8}B decay is measured by the CC reaction rate, assuming no spectral distortion. Comparison of $\phi^{\rm CC}(\nu_e)$ to the value of $\phi^{\rm NC}(\nu_x)$ provides a null hypothesis test for neutrino flavor change. The flux of active neutrinos or anti-neutrinos other than electron neutrinos inferred from these two measurements yields a 5.3σ difference, assuming the systematic uncertainties are normally distributed, providing clear evidence that there is a non-electron neutrino flavor active component in the solar flux.

Figure 3 (a) displays the distribution obtained by SNO for $\cos\theta_{\odot}$, the angle between the reconstructed direction of the event and the instantaneous direction from the Sun to the Earth. The forward peak in this distribution arises from the

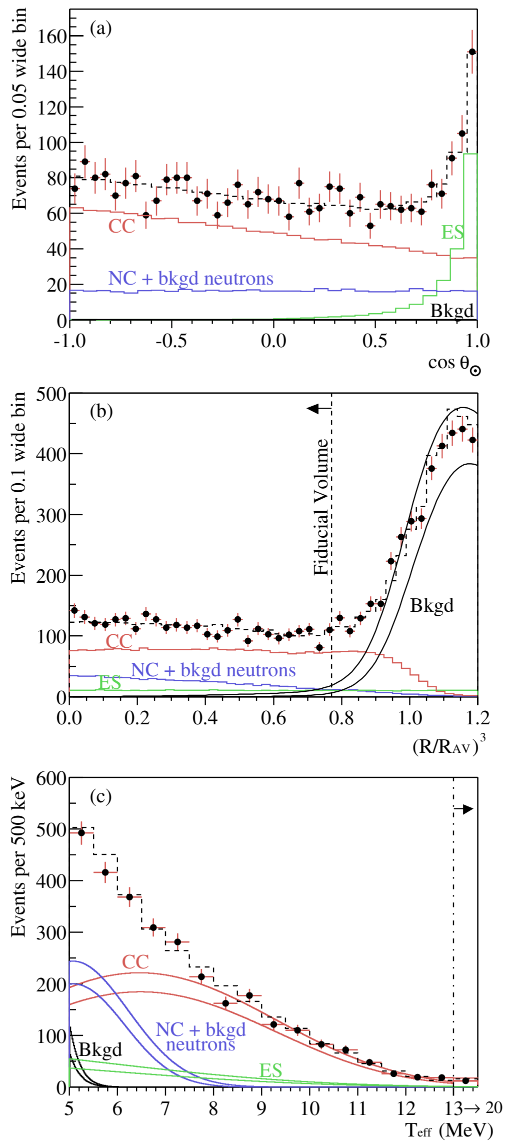

Figure 3: (a) Distribution of $\cos\theta_{\odot}$ for $R \leq 550$ cm. (b) Distribution of the volume weighted radial variable $(R/R_{\mathrm{AV}})^3$. (c) Kinetic energy for $R \leq 550$ cm. Also shown are the Monte Carlo predictions for CC, ES and NC + bkgd neutron events scaled to the fit results, and the calculated spectrum of Cherenkov background (Bkgd) events. The dashed lines represent the summed components, and the bands show $\pm 1\sigma$ uncertainties. All distributions are for events with $T_{\mathrm{eff}} \geq 5$ MeV.

kinematics of the ES reaction, while CC electrons are expected to have a distribution which is $(1 - 0.340 \cos\theta_{\odot})$ [13], before accounting for detector response.

Normalized to the integrated rates above the kinetic energy threshold of

$T_{\rm eff}\geq$ 5 MeV, the flux of ^{8}B neutrinos measured with each reaction in SNO, assuming the standard spectrum shape [14] is (all fluxes are presented in units of 10^6 cm^{-2}s^{-1}):

$$\begin{aligned}
\phi^{\rm SNO}_{\rm CC} &= 1.76^{+0.06}_{-0.05}({\rm stat.})^{+0.09}_{-0.09}\ ({\rm syst.}) \\
\phi^{\rm SNO}_{\rm ES} &= 2.39^{+0.24}_{-0.23}({\rm stat.})^{+0.12}_{-0.12}\ ({\rm syst.}) \\
\phi^{\rm SNO}_{\rm NC} &= 5.09^{+0.44}_{-0.43}({\rm stat.})^{+0.46}_{-0.43}\ ({\rm syst.}).
\end{aligned}$$

Electron neutrino cross sections are used to calculate all fluxes. The excess of the NC flux over the CC and ES fluxes implies neutrino flavor transformations. The result for the total active neutrino flux obtained with the NC reaction is in very good agreement with the value calculated [2] by solar models: $5.05 \pm 1.0 \times 10^6$ cm^{-2}s^{-1}.

A simple change of variables resolves the data directly into electron (ϕ_e) and non-electron ($\phi_{\mu\tau}$) components. This change of variables allows a direct test of the null hypothesis of no flavor transformation ($\phi_{\mu\tau} = 0$) without requiring calculation of the CC, ES, and NC signal correlations.

$$\begin{aligned}
\phi_e &= 1.76^{+0.05}_{-0.05}({\rm stat.})^{+0.09}_{-0.09}\ ({\rm syst.}) \\
\phi_{\mu\tau} &= 3.41^{+0.45}_{-0.45}({\rm stat.})^{+0.48}_{-0.45}\ ({\rm syst.})
\end{aligned}$$

assuming the standard ^{8}B shape. Combining the statistical and systematic uncertainties in quadrature, $\phi_{\mu\tau}$ is $3.41^{+0.66}_{-0.64}$, which is 5.3σ above zero, providing strong evidence for flavor transformation consistent with neutrino oscillations [15, 16].

Figure 4 shows the flux of non-electron flavor active neutrinos vs the flux of electron neutrinos deduced from the SNO data. The three bands represent the one standard deviation measurements of the CC, ES, and NC rates. The error ellipses represent the 68%, 95%, and 99% joint probability contours for ϕ_e and $\phi_{\mu\tau}$.

Spectra for day and night time periods have also been obtained by SNO that show no statistically significant differences, in agreement with the previous measurements by Super-Kamiokande. If oscillation solely to a sterile neutrino is occurring, the SNO CC-derived ^{8}B flux above a threshold of 6.75 MeV will be consistent with the integrated Super-Kamiokande ES-derived ^{8}B flux above a threshold of 8.5 MeV[17]. Adjusting the ES threshold[5] this derived flux difference is $0.53\pm0.17\times10^6$ cm^{-2}s^{-1}, or 3.1σ away from zero, implying that the oscillation is not solely to sterile neutrinos. More recent results SNO [7] and Super-Kamiokande [6] with lower thresholds increase this difference to more than 4.5σ away from zero.

SNO's day and night energy spectra have also been used to produce MSW exclusion plots and limits on neutrino flavor mixing parameters [7]. MSW oscillation

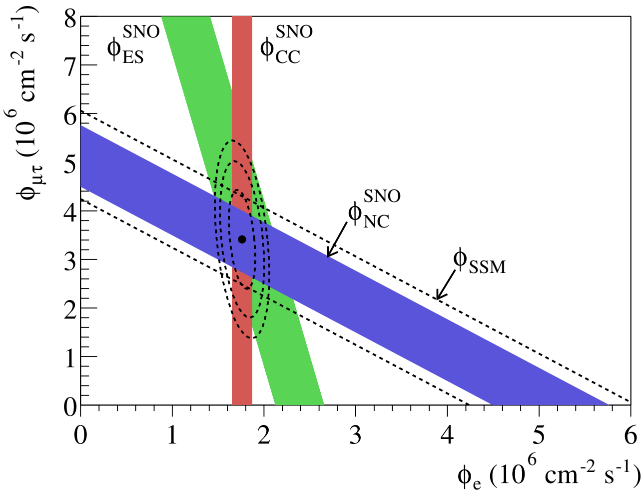

Figure 4: Flux of ^{8}B solar neutrinos which are μ or τ flavor vs flux of electron neutrinos deduced from the three neutrino reactions in SNO. The diagonal bands show the total ^{8}B flux as predicted by the SSM [2] (dashed lines) and that measured with the NC reaction in SNO (solid band). The intercepts of these bands with the axes represent the $\pm 1\sigma$ errors. The bands intersect at the fit values for ϕ_e and $\phi_{\mu\tau}$, indicating that the combined flux results are consistent with neutrino flavor transformation assuming no distortion in the ^{8}B neutrino energy spectrum.

models between two active flavors were fit to the data. For simplicity, only the energy spectra were used in the fit, and the radial R and direction $\cos\theta_\odot$ information was omitted. This procedure preserves most of the ability to discriminate between oscillation solutions. A model was constructed for the expected number of counts in each energy bin by combining the neutrino spectrum, the survival probability, and the cross sections with SNO's response functions.

There are 3 free parameters in the fit: the total ^{8}B flux ϕ_B, the difference Δm^2 between the squared masses of the two neutrino mass eigenstates, and the mixing angle θ. The flux of higher energy neutrinos from the solar *hep* reaction was fixed at 9.3×10^3 cm^{-2} s^{-1} [2]. Contours were generated in Δm^2 and $\tan^2\theta$ for $\Delta\chi^2(c.l.) = 4.61\ (90\%), 5.99\ (95\%), 9.21\ (99\%)$, and $11.83\ (99.73\%)$.

Fig. 5(a) shows allowed mixing parameter regions using only SNO data with no additional experimental constraints or inputs from solar models. By including flux information from the Cl and Ga experiments, the day and night spectra from the SK experiment, along with solar model predictions for the more robust *pp*, *pep* and ^{7}Be neutrino fluxes [2], the contours shown in Fig. 5(b) were produced. This global analysis strongly favors the Large Mixing Angle (LMA) region, and $\tan^2\theta$

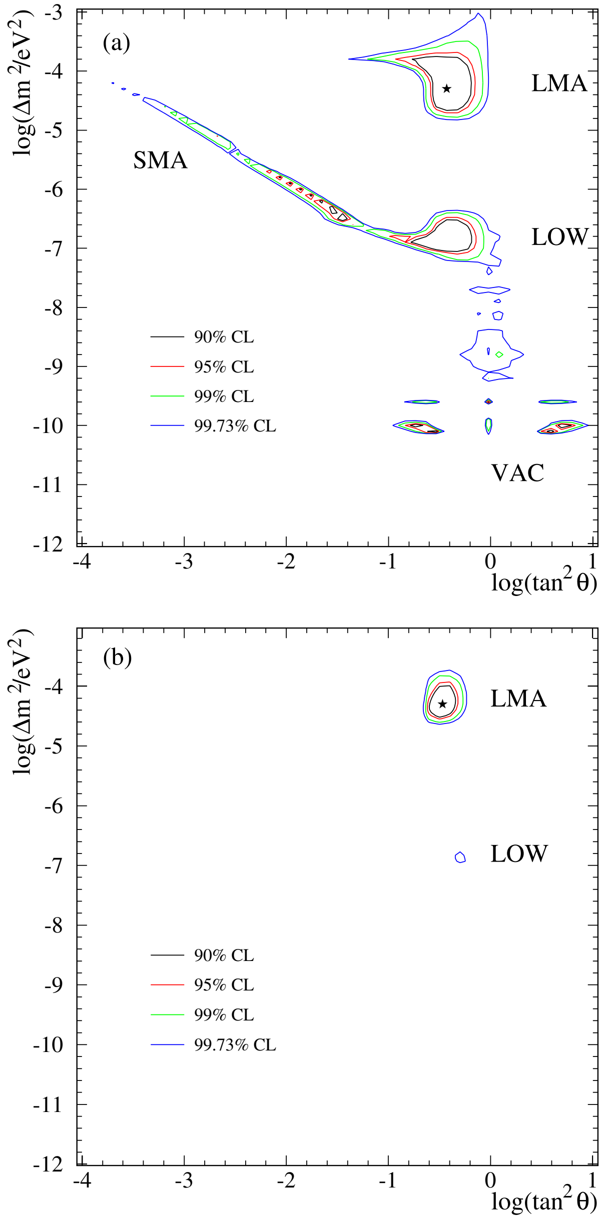

Figure 5: Allowed regions of the MSW plane determined by a χ^2 fit to (a) SNO day and night energy spectra and (b) with additional experimental and solar model data. The star indicates the best fit. See text for details.

values < 1. While the absolute chi-squared per degree of freedom is not particularly large for the LOW solution, the difference between chi-squared values still reflects the extent to which one region of MSW parameter space is favored compared to another. Repeating the global analysis using the total SNO energy spectrum instead of separate day and night spectra gives nearly identical results.

These results have been analyzed by many other authors. In general, only the LMA, LOW and in some cases the VAC regions remain at the 3 sigma level, with the LMA region strongly favored. The authors of reference [18] have shown an upper limit of about 33% for the possible sterile neutrino flux from the sun.

2 Future Measurements

All of the experiments with data to date plan to continue with solar neutrino measurements. Kamiokande has been converted to the Kamland experiment by the addition of liquid scintillator and will have a lower threshold. The Chlorine, GNO and Sage experiments will add to the accuracy of their measurements by further counting and will improve upon the determination of the low energy region of the solar neutrino spectrum. Super-Kamiokande is in the process of re-filling the detector after reinstalling the remaining phototubes following the major implosion last year. The community was shocked by the accident that befell the Super-Kamiokande experiment in November, 2001 and is very hopeful that the efforts now in progress will re-establish the capability of this great experiment as soon as possible.

The SNO experimental plan calls for three phases where different techniques are employed for the detection of neutrons from the NC reaction on deuterium. The NC reaction has a threshold of 2.2 MeV and is observed through the detection of neutrons by the three different techniques. During the first phase, with pure heavy water, neutrons were observed through the Cerenkov light produced when neutrons are captured in deuterium, producing 6.25 MeV gammas. In this phase, the capture probability for such neutrons is about 25% and the Cerenkov light is relatively close to the threshold of about 5 MeV electron energy, imposed by radioactivity in the detector. For the second phase, started in June, 2001, about 2.5 tonnes of NaCl were added to the heavy water and neutron detection is enhanced through capture on Cl, with about 8.6 MeV gamma energy release and about 83% capture efficiency. For the third phase, due to begin in 2003, the salt will be removed and an array of ^3He- filled proportional counters will be installed to provide direct detection of neutrons with a capture efficiency of about 45%. With the added sensitivity to neutrino types other than electron neutrinos via the NC reaction, the accuracy for the determination of neutrino flavor change will be increased significantly.

There are many other experiments planned in the future to provide measurements of solar neutrinos with lower energy thresholds in real time. The Kamland experiment will report results soon and could have the capability to observe ^{7}Be neutrinos. The BOREXINO experiment should also have the capability for observing ^{7}Be neutrinos and could have lower radioactive backgrounds in that region. A comprehensive summary of other planned low-energy solar neutrino measurements has been presented by S. Schonert at the Neutrino 2002 conference.

Many authors have analyzed the future capabilities of the existing experiments for restricting the allowed regions of parameter space in future. A major restriction on oscillation parameters for active neutrinos could be provided by the results from the Kamland experiment for reactor neutrinos if the correct solution is LMA. When these results are combined with the SNO results, significant restrictions can be placed on sterile neutrinos without reliance on solar model calculations [18]. Initial solar fluxes of electron neutrinos can also be determined with high accuracy through the combination of these experimental results.

In summary, the set of solar neutrino experiments to date have provided a clear picture of neutrino properties and definitive tests of solar models. The future measurements show excellent promise for a fuller understanding of neutrino and solar properties as these and other experiments proceed.

References

1. B. T. Cleveland *et al.*, Astrophys. J. **496**, 505 (1998).
2. J.N. Bahcall, M.H. Pinsonneault, and S. Basu, astro-ph/0010346 v2 (2001).
3. A.S. Brun, S. Turck-Chièze, and J.P. Zahn, Astrophys. J. **525**, 1032 (1999); S. Turck-Chièze *et al.*, Ap. J. Lett., v. **555** July 1, 2001.
4. L. Wolfenstein, Phys. Rev. D17 (1978) 2369; S.P. Mikheyev and A.Y. Smirnov, Sov. Jour. Nucl. Phys. 42 (1985) 913.
5. S. Fukuda *et al.*, Phys. Rev. Lett. **86**, 5651 (2001).
6. S. Fukuda *et al.*, hep-ex/0205075.
7. The SNO Collaboration, Phys. Rev. Lett. **89**, 011301 and 011306 (2002).

8. The SNO Collaboration, Phys. Rev. Lett. **87**, 071301 (2001).

9. K.S. Hirata *et al.*, Phys. Rev. Lett. **65**, 1297 (1990); K.S. Hirata *et al.*, Phys. Rev. **D44**, 2241 (1991); K.S. Hirata *et al.*, Phys. Rev. **D45**, 2170E (1992); Y. Fukuda *et al.*, Phys. Rev. Lett. **77**, 1683 (1996). This is the combined results from Kamiokande II and III.

10. V. N. Gavrin, reported at Neutrino 2002 Conference, Munich, May, 2002.

11. W. Hampel *et al.*, Phys. Lett. **B447**, 127 (1999). This is the combined results from GALLEX I, II, III, and IV.

12. T. Kirsten, reported at Neutrino 2002 conference, Munich, May 2002.

13. J.F. Beacom and P. Vogel, hep-ph/9903554, Phys. Rev. Lett. **83**, 5222 (1999).

14. C.E. Ortiz *et al.*, Phys. Rev. Lett. **85**, 2909 (2000).

15. Z. Maki, N. Nakagawa, and S. Sakata Prog. Theor. Phys. **28**, 870 (1962).

16. V. Gribov and B. Pontecorvo Phys. Lett. **B28**, 493 (1969).

17. G. L. Fogli, E. Lisi, A. Palazzo, and F.L. Villante Phys. Rev. D **63**, 113016 (2001); F.L. Villante, G. Fiorentini and E. Lisi Phys. Rev. D **59** 013006 (1999).

18. J. N. Bahcall, M.C. Gonzales-Garcia and C. Pena-Garay hep-ph/0204194.